Modification of Monomolecular Self-Assembled Films by Nitrogen−Oxygen Plasma

Chih-Chiang Weng,[†] Jiunn-Der Liao,*[,†] Yi-Te Wu,[†] Ming-Chen Wang,[†] Ruth Klauser,[‡] and Michael Zharnikov*[,§]

Department of Materials Science and Engineering, National Cheng Kung University, No. 1, University Road, Tainan 70101, Taiwan, National Synchrotron Radiation Research Center, 101 Hsin-Ann Road, Hsinchu 30077, Taiwan, and Angewandte Physikalische Chemie, Universität Heidelberg, Im Neuenheimer Feld 253, 69120 Heidelberg, Germany

Received: January 26, 2006; In Final Form: May 2, 2006

The modification of octadecanethiolate self-assembled monolayers on Au and Ag by nitrogen−oxygen downstream microwave plasma with variable oxygen content (up to 1%) has been studied by synchrotron-based high-resolution X-ray photoelectron spectroscopy. The primary processes were dehydrogenation, desorption of hydrocarbon and sulfur-containing species, and the oxidation of the alkyl matrix and headgroup−substrate interface. The exact character and the rates of the plasma-induced changes were found to be dependent on the substrate and plasma composition, with the processes in the aliphatic matrix and headgroup−substrate interface being mostly decoupled. In particular, the rates of all major plasma-induced processes were found to be directly proportional to the oxygen content in the plasma, which can be, thus, considered as a measure of the plasma reactivity. Along with the character of the observed changes, exhibiting a clear dominance of the oxidative processes, this suggests that the major effect of the oxygen−nitrogen downstream microwave plasma is provided by reactive oxygen-derived species in the downstream region, viz. long-living oxygen radicals and metastable species.

1. Introduction

A precise control over surface properties of materials on different length scales represents an important scientific and technological issue. In this regard, a perspective approach is the functionalization of the relevant surfaces by self-assembled monolayers (SAMs). These films are usually comprised of long-chain molecules, which are chemically bonded to the substrate via their headgroup while the molecular chain (spacer) terminated by a definite functional group points away from the substrate.[1−3] Such an arrangement results in a well-ordered and densely packed monomolecular film, giving the surface a new chemical identity, which is mostly determined by the character of the terminal functional group.

If necessary, SAMs can be additionally modified by physical means, including electron-,[4−17] X-ray-,[16,18−22] or UV-irradiation,[23−27] ion bombardment,[28] local oxidation,[29] or plasma treatment,[30−35] which results in a further change of surface properties. The treatment can be applied either to the entire surface or locally, which enables the creation of conventional and chemical lithographic patterns on the SAM basis.

Among the aforementioned physical methods, plasma processing has attracted less attention, even though several successive attempts of etching[30] and chemical modification[31] of SAMs by plasma have been reported. The difficulty in applying plasma is mostly related to the complexity of the respective phenomena, since plasma emits light of different wavelengths and comprises different reactive species, including neutral and ionized particles, high- or low-energy electrons, metastable species, and free radicals. The impact of the individual species and the general effect of the plasma depend on its type and energy content and are often difficult to predict and monitor in detail. Generally, the main effect is caused by high-energy electrons and ions. However, in the case of soft materials and especially ultrathin organic films, it can be of advantage to reduce or even avoid the effect of these high-energy moieties and put emphasis on low-energy species. Such a situation can be, e.g., achieved in the afterglow region of downstream plasma, which is frequently chosen for the purpose of surface cleaning, etching, or modification. The amount of high-energy electrons and ions in such a plasma is massively reduced on the way from the excitation area to the afterglow region. The dominant plasma constituents in this area are long-living free radicals and some metastable species; they provide the major effect, along with the ultraviolet light emitted by the excited species.[36,37]

Recently, we used a nitrogen−oxygen and argon−oxygen microwave downstream plasma for the modification of aliphatic and aromatic thiol-derived SAMs on Au and Ag substrates.[32−35] The plasma treatment resulted in significant changes of these films, leading to the oxidation of the hydrocarbon matrix and the thiolate headgroups, with the subsequent desorption of the alkanesulfonate species. The rates and extent of these processes and the exact mechanism of film modification depended on the substrate and the length of the SAM constituent. However, the experiments suffered from an ambiguity of the plasma composition, since oxygen, which provided the major effect, was introduced into the plasma in a noncontrolled way, presumably originating from the walls of the reactor and the quartz tube.

In this study, we intentionally introduced a definite portion of oxygen into the nitrogen plasma and monitored the influence of the plasma composition on the effect of the downstream

* Corresponding authors. E-mail: jdliao@mail.ncku.edu.tw (J.-D.L.); Michael.Zharnikov@urz.uni-heidelberg.de (M.Z.). Phone: (886) 6 2749140 (J.-D.L.). Fax: (886) 6 2346290 (J.-D.L.).

[†] National Cheng Kung University.

[‡] National Synchrotron Radiation Research Center.

[§] Universität Heidelberg.

10.1021/jp060572r CCC: $33.50
Published on Web 06/03/2006

nitrogen−oxygen plasma on thiol-derived SAMs. As a test system, we chose such widely known systems as SAMs of *n*-octadecanethiol (ODT: $CH_3(CH_2)_{17}SH$) on the evaporated Au(111) and Ag(111) substrates.

In the following section, we will give a brief description of the experimental procedure. Thereafter, the results are presented and preliminarily discussed in section 3. An extended analysis of the data is given in section 4, following by a summary in section 5.

2. Experimental Section

2.1. Sample Preparation. Au and Ag substrates were prepared by thermal evaporation of 200 nm of Au or 100 nm of Ag (99.99% purity) onto the polished single-crystal silicon (100) wafers (Silicon Sense) primed with a 5 nm titanium adhesion layer. Such evaporated films are standard substrates for thiol-derived SAMs. They are polycrystalline, with a grain size of 20−50 nm as observed by atomic force microscopy. The grains predominantly exhibit a (111) orientation.[38,39] The SAMs were formed by immersion of freshly prepared substrates into a 1 mmol solution of ODT in absolute ethanol at room temperature for 24 h. After immersion, the samples were carefully rinsed with pure ethanol, blown dry with argon, and kept for several days in argon-filled glass containers until the characterization. No evidence for impurities or oxidative degradation products was found.

2.2. Plasma Treatment. Plasma treatment was performed in a custom-made preparation chamber, which was carefully cleaned before the experiments. The ODT samples were fixed on the sample holder in front of the outlet of a quartz tube with an inner diameter of 5 mm leading to the plasma glow discharge region. The distance between the sample surface and this region was ≈170 mm while the spacing between the sample and nozzle head was ≈10 mm. The glow discharge microwave plasma was produced using a microwave plasma generator (OPTHOS Instruments Inc.) with a frequency of ≈2.45 *G*Hz and a power of 80 W. A flow rate of 500 sccm for nitrogen/oxygen gas (purity of 99.9999%) was maintained by keeping a pressure of ≈1 Torr in the plasma processing chamber. The respective pressure in the gas-discharged region was ≈13 Torr. The oxygen content was varied from 0 to 1% in a step of 0.25%. The plasma treatment time was carried out for fixed time intervals of 15−105 s in a step of 15 s to follow the sample modification in detail.

In the case of "pure" nitrogen plasma there were oxygen-derived species in the afterglow region, even though the preparation chamber was baked and high-purity nitrogen was used and purged for several times before the experiments. We assume that these species originated from the walls of the reactor and the quartz tube.

2.3. Characterization of the Plasma. The afterglow plasma in the vicinity of the sample was characterized using a Langmuir probe connected to an electrometer (Keithley, model 6514). This invasive, electrostatic probe utilizes a 10 mm long tungsten wire of 0.25 mm diameter as the probing tool. Using the $I-V$ curves measured by this device, plasma density, the electron temperature, and plasma sheath-induced potential were calculated according to the standard equations.[32] A simplified model within the framework of so-called thin sheath theory has been used.[32,40−42] On the basis of this model, the electron/ion density in the afterglow region was estimated as $(1.38 \pm 0.26) \times 10^6$ particles/cm^3 for the nitrogen/oxygen plasma, which corresponds to a low kinetic energy of electrons of ≈0.5 eV and an electron temperature of ≈5500 K.

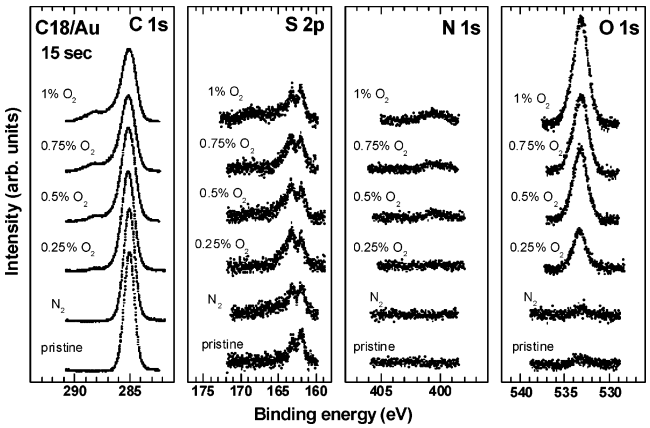

Figure 1. C 1s, S 2p, N 1s, and O 1s HRXPS spectra of pristine (bottom curves) and plasma-processed ODT/Au. The duration of the plasma exposure was 15 s. The spectra are labeled by the corresponding oxygen content in the plasma.

2.4. Sample Characterization by HRXPS. The characterization of the pristine and plasma-treated films was performed by synchrotron-based high-resolution X-ray photoelectron spectroscopy (HRXPS) using a spectroscopy branch of the U5 undulator beamline at the National Synchrotron Radiation Research Center in Hsinchu, Taiwan. The sample transfer from the preparation chamber to the analysis position occurred without its exposure to air. The spectra were acquired with a CLAM-4 electron energy analyzer (VG Microtech). For both pristine samples and films treated by the plasma, wide scan, Au 4f, Ag 3d, S 2p, C 1s, O 1s, and N 1s spectra were collected. The Au 4f, S 2p, and C 1s spectra were acquired at an excitation energy of 390 eV while the wide scan, Ag 3d, N 1s, and O 1s spectra were measured at a photon energy of 650 eV. The energy resolution was 0.25−0.3 eV. The energy scale was referenced to the pronounced Au $4f_{7/2}$ peak of ODT/Au at 84.00 eV.[39,43] The energy calibration was performed for every sample and after every change of the photon energy or beamline slits to exclude any instability or a drift. The spectra acquisition time was selected in such a way that no noticeable damage by the primary X-rays occurred during the measurements.[16,19−21]

The HRXPS spectra were decomposed into individual components by a consistent fitting procedure using Voigt peak profiles and a Shirley background. To fit the S $2p_{3/2,1/2}$ doublet, we used two such peaks with the same fwhms, a standard[43] spin−orbit splitting of ca. 1.2 eV (verified by the fit), and a branching ratio of 2:1 (S $2p_{3/2}$/S $2p_{1/2}$). The resulting accuracy of the BE values is ca. 0.05 eV.

Film thickness evaluation was performed on the basis of the Au 4f and C 1s intensities assuming an exponentional attenuation of the photoelectron signal. The attenuation lengths were taken in accordance with ref 44, in which these values were precisely measured over a wide range of photon energies.

3. Results

The S 2p, C 1s, N 1s, and O 1s HRXPS spectra of the pristine and plasma-processed ODT/Au are presented in Figures 1 and 2 for a treatment time of 15 and 45 s, respectively. The analogous spectra of ODT/Ag are depicted in Figures 3 and 4. These selected spectra should give a visual impression about the plasma-induced changes in the ODT SAMs as well as illustrate the effects of the substrate and oxygen content in the plasma.

The results of the decomposition (see an example in Figure 5) and analysis of the entire spectra set are presented in Figures

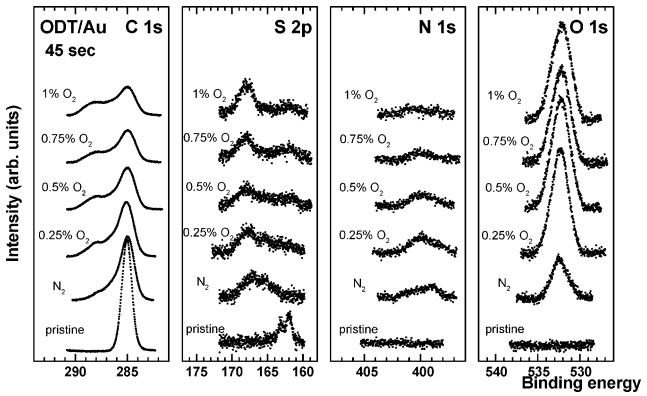

Figure 2. C 1s, S 2p, N 1s, and O 1s HRXPS spectra of pristine (bottom curves) and plasma-processed ODT/Au. The duration of the plasma exposure was 45 s. The spectra are labeled by the corresponding oxygen content in the plasma.

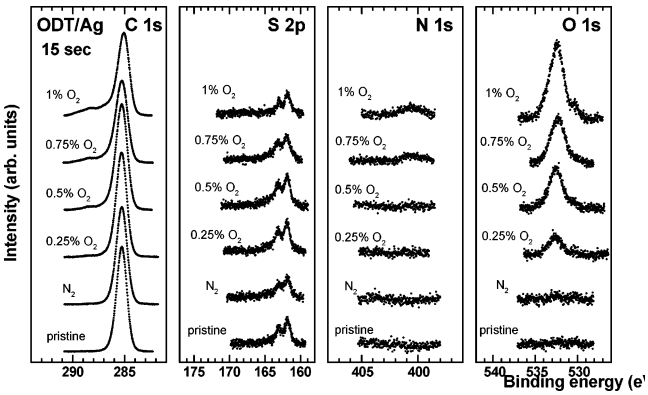

Figure 3. C 1s, S 2p, N 1s, and O 1s HRXPS spectra of pristine (bottom curves) and plasma-processed ODT/Ag. The duration of the plasma exposure was 15 s. The spectra are labeled by the corresponding oxygen content in the plasma.

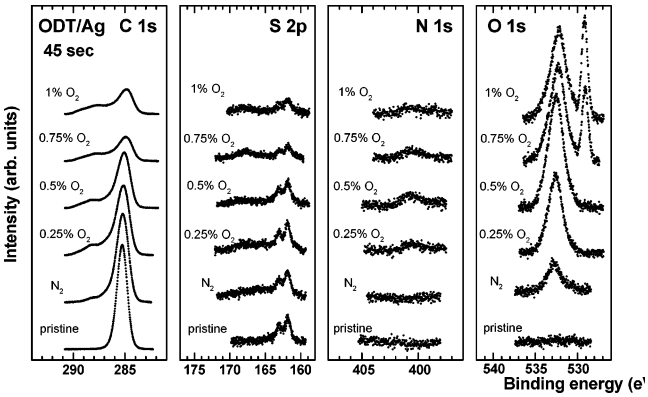

Figure 4. C 1s, S 2p, N 1s, and O 1s HRXPS spectra of pristine (bottom curves) and plasma-processed ODT/Ag. The duration of the plasma exposure was 45 s. The spectra are labeled by the corresponding oxygen content in the plasma.

6−10, in which total C 1s (Figure 7), S 2p (Figure 9), and O 1s (Figure 10) intensities as well as the intensities related to the intact aliphatic chains (Figure 6) and oxidized hydrocarbon species (Figure 8) are depicted as a function of plasma treatment time. The assignments of the individual emissions are given in Tables 1−4. Note that the intensity related to the intact aliphatic chains can only be considered as a tentative parameter, since it is difficult to distinguish the respective signal in the C 1s spectra; we just used the intensity of the main peak.

The C 1s spectra of the pristine films exhibited a single emission peak at a BE of 284.9 eV (Au) and 285.2 (Ag), with

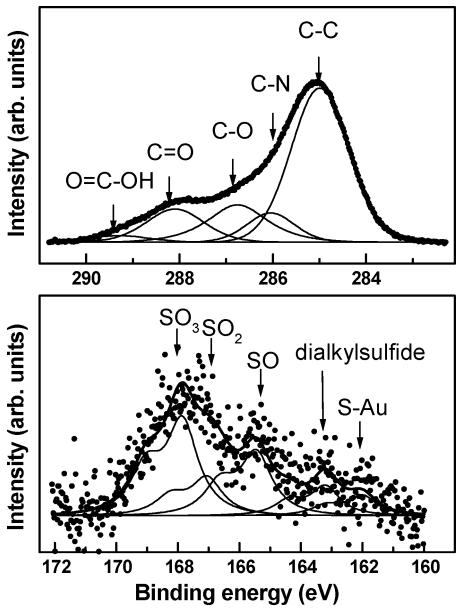

Figure 5. An example for the decomposition of the C1s and S 2p HRXPS spectra. The data for ODT/Au exposed to the plasma with an oxygen content of 0.25% for 45 s are shown.

TABLE 1: Assignments of the Individual Emissions in the C 1s HRXPS Spectra

peak assignment	C−C (Au/Ag)	C−N	C−O	C═O	O═C−O
binding energy (eV)	285.0/285.3	286.0	286.8	288.3	289.3

TABLE 2: Assignments of the Individual Emissions in the S 2p HRXPS Spectra

peak assignment	S−Au	dialkyl sulfide	SO	SO_2	SO_3
binding energy (eV)	162.0	163.2	165.5	166.9	167.8

TABLE 3: Assignments of the Individual Emissions in the O 1s HRXPS Spectra

peak assignment	Ag_2O	C═O, O═C−O	SO_2, SO_3	NO
binding energy (eV)	529.15	532.2	532.0−532.5	533.3

TABLE 4: Assignments of the Individual Emissions in the N 1s HRXPS Spectra

peak assignment	nitride	O−N and N−H	C−N
binding energy (eV)	398.4	400	401.5

a fwhm of ≈0.9 eV in good agreement with previous HRXPS studies.[39,45,46] No traces of oxygen or nitrogen were found as shown by the respective O 1s and N 1s spectra. The S 2p spectrum of both ODT/Au and ODT/Ag exhibited a single S 2p doublet with a BE of ≈162.0 eV for the S $2p_{3/2}$ component. This doublet is commonly related to the thiolate species bonded to Au surface.[39,47] No traces of other sulfur-derived species such as, e.g., atomically adsorbed or differently (from thiolate) bonded sulfur (161.0 eV for S $2p_{3/2}$),[48−50] irradiation-induced dialkyl sulfide species (163.4 eV for S $2p_{3/2}$),[21] or oxidized sulfur (165.5−169.8 eV for S $2p_{3/2}$)[34,51,52] were found.

The spectra of ODT/Au and ODT/Ag exhibited pronounced changes in the course of the plasma exposure, reflecting transformation and desorption processes in the monomolecular films. In the C 1s spectra, the total C 1s intensity and the intensity of the C 1s peak related to the intact alkyl chains (i.e. the main peak) decreased, a downward shift and broadening of

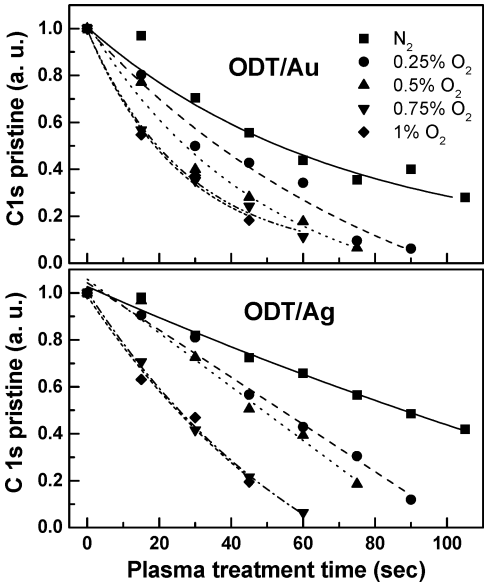

Figure 6. C 1s intensity related to the intact aliphatic chains for pristine and plasma-processed ODT/Au (top panel) and ODT/Ag (bottom panel) as function of the plasma treatment time. The oxygen content in the plasma was varied. The intensity is normalized to the value for the pristine SAMs.

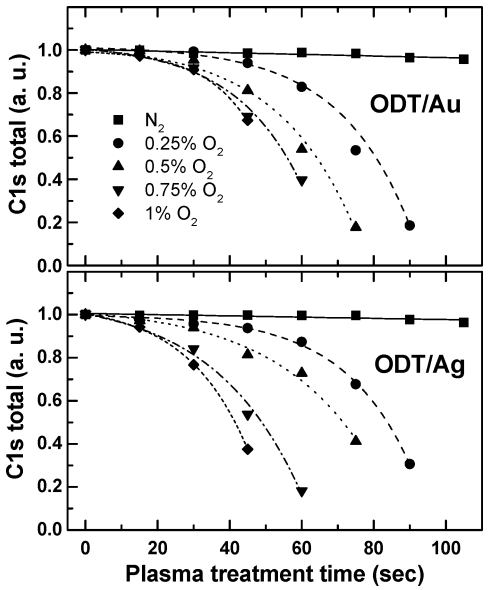

Figure 7. C 1s total intensity for pristine and plasma-processed ODT/Au (top panel) and ODT/Ag (bottom panel) as function of the plasma treatment time. The oxygen content in the plasma was varied. The intensity is normalized to the value for the pristine SAMs.

this peak occurred (following dehydrogenation), and a variety of new features on the high BE side of the main emission evolved. These new features can be mostly assigned to different oxygen-containing moieties, with a dominant contribution from C═O species. The observed changes imply disordering, decomposition, dehydrogenation, and oxidation of the alkyl matrix in the course of the plasma treatment (note that not all these processes can be *directly* monitored by the C 1s HRXPS spectroscopy but have been clearly evidenced by other techniques; see ref 16 and references therein). According to the data presented in Figures 6 and 7, both damage of the intact aliphatic chains and desorption of hydrocarbon fragments occur continuously in the course of the plasma treatment. These processes are accompanied by continuous oxidation of the alkyl matrix, which follows from the observed increase of the respective

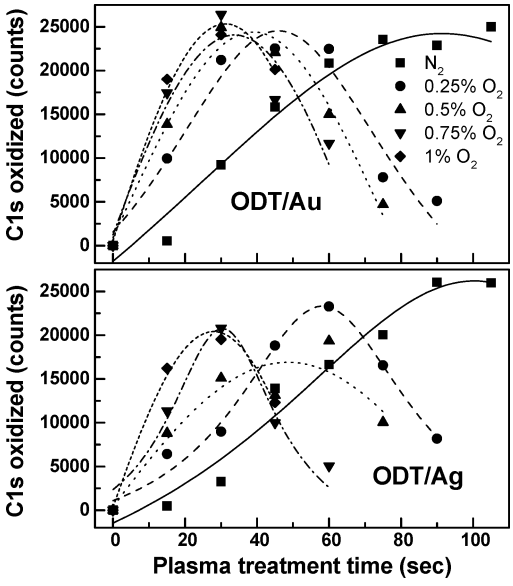

Figure 8. C 1s intensity related to oxygen-containing species in pristine and plasma-processed ODT/Au (top panel) and ODT/Ag (bottom panel) as function of the plasma treatment time. The oxygen content in the plasma was varied.

photoemission signal at the initial stage of the plasma treatment, as shown in Figure 8. With the progressive desorption of both hydrocarbon and oxidized species in the course of the further plasma treatment, the signal from the oxidized species started to decrease (except for the N_2 plasma), so that a peaklike dependence of the corresponding intensity as a function of treatment time was observed (see Figure 8).

In the S 2p spectra, the doublet related to the pristine thiolate species decreased in intensity while the emissions related to dialkyl sulfides, sulfenates (165.5 eV for S $2p_{3/2}$), sulfinates (166.9 eV for S $2p_{3/2}$), and sulfonates (167.6 eV for S $2p_{3/2}$) evolved and even became dominating (only for ODT/Au). These changes can be associated with a cleavage of the pristine S−Au bonds and the oxidation of the emerging species to sulfinates and sulfonates. According to the S 2p spectra in Figure 2, this is a dynamical process, so that the average oxidation state of the sulfur-derived species increased continuously with the exposure time. The emerging dialkyl sulfonate and SO_n species were not necessarily located at the SAM−substrate interface but could be distributed over the film. The respective photoelectron signals underwent, therefore, a lower attenuation as compared to that for the pristine thiolate species, which partly explains the observed increase in the S 2p total intensity at the initial stage of the plasma treatment, as shown in Figure 9. Another reason for this intensity increase is the film thinning, associated with the desorption of the hydrocarbon species originated from the alkyl matrix (see above). With the progressive plasma treatment, not only hydrocarbon but also sulfur-containing species desorb, which result in a decrease of the total S 2p intensity, so that a peaklike dependence of this signal as a function of treatment time was observed, as shown in Figure 9.

The oxidation of the alkyl matrix and the thiolate groups is accompanied by the appearance of the corresponding emissions in the O 1s spectra, with a dominance of the contributions from the C−O, C═O, and O═C−O species in the alkyl matrix at 532.5−532.15 eV (the respective peak shifts slightly to lower BE during the plasma treatment, following the progressive development of C═O and O═C−O bonds). This conclusion directly follows from the combined analysis of the C 1s, S 2p,

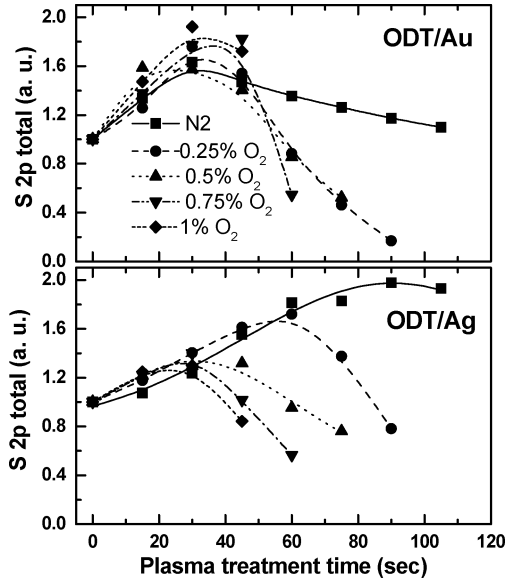

Figure 9. S 2p total intensity for pristine and plasma-processed ODT/Au (top panel) and ODT/Ag (bottom panel) as function of the plasma treatment time. The oxygen content in the plasma was varied. The intensity is normalized to the value for the pristine SAMs.

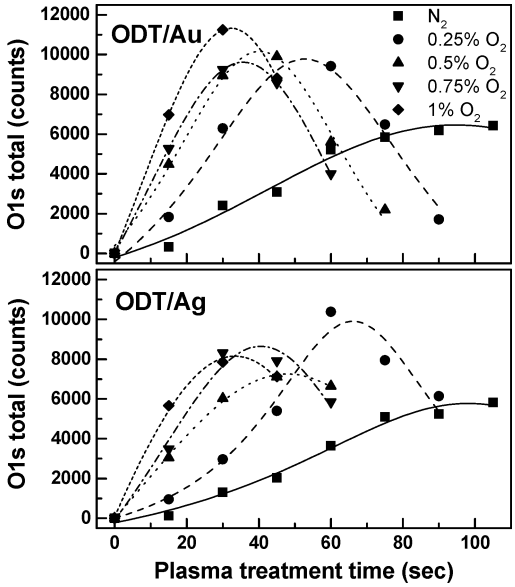

Figure 10. O 1s total intensity for pristine and plasma-processed ODT/Au (top panel) and ODT/Ag (bottom panel) as function of the plasma treatment time. The oxygen content in the plasma was varied.

and O 1s spectra (see, e.g., Figure 4)—there is a noticeable O 1s signal, even though the extent of the oxidation of the thiolate species is quite low. The other evidence is the similarity in the behavior of the C 1s (oxidized species) and O 1s signals as a function of the plasma treatment time, as directly follows from the comparison of the Figures 8 and 10. The only distinct difference is the lesser drop of the total O 1s intensity at long treatment time as compared to the C 1s signal originating from the oxidized hydrocarbon species in the case of ODT/Ag. This difference can be, however, explained by the oxidation of the Ag substrate (the respective emission at 529.15 eV is observed in the O 1s spectra), which results in the appearance of the additional contribution in the total O 1s signal and partly compensates the intensity decrease related to desorption.

In contrast to the strong O 1s signal, only weak N 1s intensity is observed in the respective HRXPS spectra of the plasma-

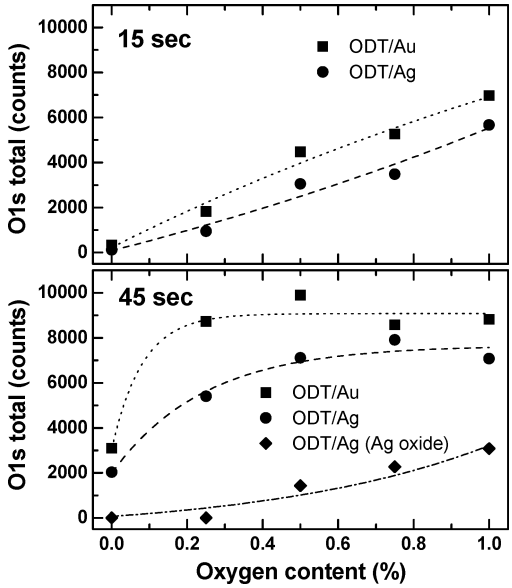

Figure 11. O 1s total intensity for plasma-processed ODT/Au (squares) and ODT/Ag (circles) as function of the oxygen content in the plasma. Also, the intensity of the O 1s signal related to the oxidation of the Ag substrate is presented (diamonds). The duration of the plasma exposure was 15 s (top panel) and 45 s (bottom panel).

treated ODT SAMs. The emissions can be related to C−N and O−C−N species at a BE of 399−401 eV. There is no clear correlation between the changes of the O 1s and N 1s spectra during the plasma treatment.

The extent and exact course of the observed changes upon the plasma treatment depend on the substrate and oxygen content of the plasma. As for the substrate effect, the films on Ag are obviously more resistant to degradation by the reactive plasma, which is mostly related to stronger thiolate−metal and sulfonate−metal bonds as compared to those on Au.[34] In particular, this can be directly seen, if one compares the S 2p spectra in Figures 2 and 4: whereas most of the thiolate species of ODT/Au transformed to sulfonates, a noticeable part of the thiolate species in ODT/Ag was still intact after the plasma treatment for 45 s. At the same time, apart from the thiolate−substrate interface, overall degradation of the ODT films of this study was not significantly slower on Ag than on Au.

The effect of the oxygen content in the plasma is clearly seen from the comparison of the C 1s, S 2p, N 1s, and O 1s spectra within the individual panels of Figures 1−4 and from the behavior of the individual photoemission signals in Figures 6−10. The effect is additionally illustrated by Figure 11, where the total intensity of the O 1s signal and the O 1s intensity related to the oxidation of the Ag substrate are presented for the ODT SAMs exposed to the nitrogen−oxygen plasma of variable composition for 15 and 45 s. According to this figure, the rate of the oxidation of the alkyl matrix at the initial stage of the plasma treatment (e.g., for 15 s) is directly proportional to the oxygen content. This is also true for the alkyl chain damage (Figure 6) and desorption processes (Figure 7), which occur in parallel. At the further treatment (e.g., for 45 s), the linear relation between the extent of oxidation in the SAMs and oxygen content in the plasma was distorted (see Figure 11), and the combination of the oxidation and desorption processes resulted in complex, peaklike behavior of the photoemission intensities related to the oxidative species as shown in Figures 8−10.

In contrast to the alkyl matrix, the character and extent of the plasma-induced processes at the thiolate−substrate interface depends only slightly on the plasma composition and is mostly

determined by the identity of the substrate. On the Au substrate (see Figures 1 and 2), a fast oxidation of the pristine thiolate species occurs during the plasma exposure, so that no such species remain after a prolonged treatment (see Figure 2). On the Ag substrate, thiolate species are practically unaffected by the oxidation processes at the initial stage of the plasma treatment (see Figure 3), with a noticeable part staying intact upon a prolonged exposure to the plasma (see Figure 4). The analysis of the S 2p spectra in Figures 3 and 4 shows that not only the oxidation but the desorption processes are mostly responsible for the kinetics of the thiolate species in the case of Ag. In accordance, the rate of the oxidation of the Ag substrate, which becomes exposed to reactive oxygen-containing moieties after desorption of the headgroup-related species, is proportional to the oxygen content in the plasma, as shown in the lower panel of Figure 11.

Note that oxidation processes occurred not only for the nitrogen−oxygen but also for the "pure" nitrogen plasma, which means that it was likely contaminated by oxygen. From the spectra analysis, the respective level of contamination was estimated to be far below 0.1%, which is still a noticeable amount in view of the fact that the major impact of the plasma on ODT SAMs was provided by reactive oxygen-derived species.

4. Discussion

The presented spectroscopic results imply that an exposure of the ODT SAMs to nitrogen−oxygen downstream microwave plasma causes a strong modification of this system, resulting in a structural damage and an oxidation of the initially well-defined and -ordered SAMs. The primary plasma-induced processes are dehydrogenation and decomposition of the alkyl chains, desorption of hydrocarbon fragments, disordering of the aliphatic matrix, and oxidation of this matrix, the thiolate headgroups, and the substrate (in the case of Ag).

The exact character and rates of the plasma-induced changes were found to be dependent on the substrate and plasma composition or, in other words, the plasma reactivity. In the case of the Au substrate, the damage of the alkyl matrix, including dehydrogenation, disordering, oxidation, and desorprtion, occurred in parallel with the damage of the headgroup−substrate interface, where the progressive oxidation of the thiolate species to sulfenates, sulfinates, and sulfonates took place. To some extent, the latter process went over the breaking of the S−Au bond and the formation of dialkyl sulfides.[21] In the case of Ag substrate, the damage of the alkyl matrix occurred to a similar extent as for Au, but the rate of oxidative processes at the headgroup−substrate interface was comparably low and the kinetics of the thiolate species was mostly determined by the desorption processes involving sulfur-containing species. Following the latter processes, oxidation of Ag substrate occurred.

The comparison of the above results for ODT/Au and ODT/Ag suggests that the plasma-induced processes in the aliphatic matrix and headgroup−substrate interface are mostly decoupled. The observed difference in the character and rate of the changes at the latter interface in ODT/Au and ODT/Ag can be explained by the different strengths of the thiolate−metal bond for these two substrates.[14] At the same time, the similarity in the reaction of the alkyl matrix of ODT/Au and ODT/Ag toward the plasma treatment is presumably related to the similar bulk densities of the respective matrixes.[1−3,47] The difference in the lateral packing densities and exact arrangements of the aliphatic chains in ODT/Au and ODT/Ag[1−3,47] are obviously of minor importance for the observed phenomena.

Being almost independent of the substrate, the rates of almost all plasma-induced processes are directly proportional to the oxygen content in the plasma. This is especially obvious at the initial stage of the plasma treatment, so long as a complex interplay of oxidation and desorption processes does not result in a complex behavior of the photoemission intensities. This proportionality reveals that the major effect of the nitrogen−oxygen plasma onto the ODT SAMs is caused by reactive oxygen-derived species, such as long-living oxygen radicals and atomic oxygen. In contrast to oxygen, the role of nitrogen-derived moieties is a minor one, since no important processes related to the effect of these species can be identified. There is no noticeable thickness reduction upon the exposure of the ODT SAMs to the "pure" nitrogen plasma, and the observed changes in the monomolecular films are mostly related to oxygen contamination and not to the nitrogen-derived species themselves. Also, the extent of the chemical reaction between the nitrogen-derived species and the ODT films is very low; the only observed nitrogen species in the plasma-treated SAMs were oxidative ones, i.e., were mediated by the presence of reactive oxygen moieties.

Apart from oxygen- and nitrogen derived radicals and metastable species, there were other components of the plasma, which could make an effect on the ODT SAMs, viz. ions, electrons, and UV radiation. As for the latter factor, our previous experiments have shown that photon-induced modification of an alkanethiolate SAM upon the exposure to downstream plasma is negligible, since no noticeable changes were observed when all other factors except for the UV light emitted by the plasma were removed.[35] As for electrons and ions, due to the specificity of the downstream discharge plasma, most of the excited and ionized species recombine or lose their energy by inelastic collisions with other plasma constituents or the walls of the quartz tube during their flow from the glow discharge area into the afterglow region. According to our measurements by Langmuir probe (see also ref 35), a characteristic energy associated with the plasma changes by a factor of 30−50 at going from the region of the plasma excitation to the vicinity of the sample. In particular, the threshold for the electron-induced damage of alkanethiolate SAMs is about 7 eV,[53,54] which is noticeably higher than the energy of the charged particles ($\approx$0.5 eV)[35] in the afterglow region. Also, the character of the observed changes does not look like as electron- or ion-induced modification. In the case of low-energy electrons, no oxidation of the alkyl matrix occurs and the major irradiation-induced process at the SAM−substrate interface is the thiolate−dialkyl sulfide transformation.[14,16,21] In the case of ions, the major processes are disordering and sputtering of a SAM,[28,55] with no trace of oxidative processes. Thus, both electrons and ions seem to be of minor importance, even though an effect induced by a small portion of "hot" ionizing particles, which survived along the pathway from the glow discharge area into the afterglow region, cannot be completely excluded.

5. Summary

The modification of ODT SAMs on Au and Ag by nitrogen−oxygen downstream microwave plasma with variable oxygen content (up to 1%) has been studied by synchrotron-based HRXPS. The primary processes were the loss of conformational and orientational order, dehydrogenation, desorption of hydrocarbon and sulfur-containing species, and the oxidation of the alkyl matrix and headgroup−substrate interface. The major impact was caused by the interplay of desorption and oxidation processes.

The exact character and the rates of the plasma-induced changes were found to be dependent on the substrate and plasma composition, with the processes in the aliphatic matrix and headgroup−substrate interface being mostly decoupled. Whereas the oxidative and desorption processes in the aliphatic matrix of ODT/Au and ODT/Ag occurred with similar rates, the thiolate−substrate interface of ODT/Ag was more resistant to the oxidative processes as compared to the analogous interface in ODT/Au. The latter difference was explained by the relatively stronger thiolate−metal bond in the case of Ag.

Apart from the substrate effect, the rates of all major plasma-induced processes were found to be directly proportional to the oxygen content in the plasma. Also, the character of the observed changes exhibited a clear dominance of the oxidative processes. Both these findings suggest that the major effect of the oxygen−nitrogen downstream microwave plasma is provided by reactive oxygen-derived species in the downstream region, viz. long-living oxygen radicals and metastable species. Even in the case of "pure" nitrogen plasma, the major effect was mediated by oxygen contamination, which amount was estimated to be less than 0.1%. The impact of electrons and ions was found to be negligible.

The results suggest that the reactivity of the binary-gas plasma toward a SAM can be precisely adjusted by the oxygen content, with the other, less-reactive component serving as a "background" agent.

Acknowledgment. We thank Prof. Michael Grunze (Universität Heidelberg) for the support of this work. The work has been supported by the National Science Council of ROC under Grant No. 94-2621-Z-006-002 and a NSC/DAAD Grant 94-2911-I-006-004, the German BMBF (05KS4VHA/4), and a DAAD/NSC Grant 423/rc-PPP-sr.

References and Notes

(1) Ulman, A. *An Introduction to Ultrathin Organic Films: Langmuir−Blodgett to Self-Assembly*; Academic Press: New York, 1991. Ulman, A. *Chem. Rev.* **1996**, *96*, 1533.

(2) Ulman, A., Ed. *Thin films: self-assembled monolayers of thiols*; Academic Press: San Diego, CA, 1998.

(3) Schreiber, F. *Prog. Surf. Sci.* **2000**, *65*, 151.

(4) Baer, D. R.; Engelhard, M. H.; Schulte, D. W.; Guenther, D. E.; Wang, L.-Q.; Rieke, P. C. *J. Vac. Sci. Technol.* **1994**, *A12*, 2478.

(5) Rowntree, P.; Dugal, P. C.; Hunting, D.; Sanche, L. *J. Phys. Chem.* **1996**, *100*, 4546.

(6) Seshadri, K.; Froyd, K.; A. N. Parikh, A, N.; Allara, D. L.; Lercel M. J.; Craighead, H. G. *J. Phys. Chem.* **1996**, *100*, 15900.

(7) Müller, H. U.; Zharnikov, M.; Völkel, B.; Schertel, A.; Harder, P.; Grunze, M. *J. Phys. Chem. B* **1998**, *102*, 7949.

(8) Olsen, C.; Rowntree, P. A. *J. Chem. Phys.* **1998**, *108*, 3750.

(9) Zerulla, D.; Chasse, T. *Langmuir* **1999**, *15*, 5285.

(10) Zharnikov, M.; Frey, S.; Gölzhäuser, A.; Geyer, A.; Grunze, M. *Phys. Chem. Chem. Phys.* **1999**, *1*, 3163.

(11) Heister, K.; Frey, S.; Gölzhäuser, A.; Ulman, A.; Zharnikov, M. *J. Phys. Chem. B* **1999**, *103*, 11098.

(12) Geyer, W.; Stadler, V.; Eck, W.; Zharnikov, M.; Gölzhäuser, A.; Grunze, M. *Appl. Phys. Lett.* **1999**, *75*, 2401.

(13) Eck, W.; Stadler, V.; Geyer, W.; Zharnikov, M.; Gölzhäuser, A.; Grunze, M. *Adv. Mater.* **2000**, *12*, 805.

(14) Zharnikov, M.; Frey, S.; Heister, K.; Grunze, M. *Langmuir* **2000**, *16*, 2697.

(15) Frey, S.; Rong, H.-T.; Heister, K.; Yang, Y.-J.; Buck, M.; Zharnikov, M. *Langmuir* **2002**, *18*, 3142.

(16) Zharnikov, M.; Grunze, M. *J. Vac. Sci. Technol., B* **2002**, *20*, 1793.

(17) Huels, M. A.; Dugal, P. C.; Sanche, L. *J. Chem. Phys.* **2003**, *118*, 11168.

(18) Laibinis, P. E.; Graham, R. L.; Biebuyck, H. A.; Whitesides, G. M. *Science* **1991**, *254*, 981.

(19) Jäger, B.; Schürmann, H.; Müller, H. U.; Himmel, H. J.; Neumann, M.; Grunze, M.; Wöll, Ch. *Z. Phys. Chem.* **1997**, *202*, 263.

(20) Wirde, M.; Gelius, U.; Dunbar, T.; Allara, D. L. *Nucl. Instrum. Methods Phys. Res., Sect. B* **1997**, *131*, 245.

(21) Heister, K.; Zharnikov, M.; Grunze, M.; Johannson, L. S. O.; Ulman, A. *Langmuir* **2001**, *17*, 8.

(22) Klauser, R.; Zharnikov, M.; Hong, I.-H.; Wang, S.-C.; Gölzhäuser, A.; Chuang, T. J. *J. Phys. 4* **2003**, *104*, 459.

(23) Lewis, M.; Tarlov, M. J.; Carron, K. *J. Am. Chem. Soc.* **1995**, *117*, 9574.

(24) Hutt, D. A.; Leggett, G. J. *J. Phys. Chem. B* **1996**, *100*, 6657.

(25) Hutt, D. A.; Cooper, E.; Leggett G. J. *J. Phys. Chem. B* **1998**, *102*, 174.

(26) Cooper, E.; Leggett G. J. *Langmuir* **1998**, *14*, 4795.

(27) Riely, H.; Kendall, G. K.; Zemicael, F. W.; Smith, T. L.; Yang, S. *Langmuir* **1998**, *14*, 5147.

(28) Chenakin, S. P.; Heinz, B.; Morgner, H. *Surf. Sci.* **1999**, *421*, 337.

(29) Maoz, R.; Cohen, S. R.; Sagiv, J. *Adv. Mater.* **1999**, *11*, 55.

(30) Lercel, M. J.; Craighead, H. G.; Parikh, A. N.; Seshadri, K.; Allara, D. L. *J. Vac. Sci. Technol., A* **1996**, *14*, 1844.

(31) Unger, W. E. S.; Lippitz, A.; Gross, Th.; Friedrich, J. F.; Wöll Ch.; Nick, L. *Langmuir* **1999**, *15*, 1161.

(32) Liao, J.-D.; Wang, M.-C.; Weng, C.-C.; Klauser**,** R.; Frey, S.; Zharnikov, M.; Grunze, M. *J. Phys. Chem. B* **2002**, *106*, 77.

(33) Wang, M.-C.; Liao, J.-D.; Weng, C.-C.; Klauser, R.; Frey, S.; Zharnikov, M.; Grunze, M. *J. Phys. Chem. B* **2002**, *106*, 6220.

(34) Wang, M.-C.; Liao, J.-D.; Weng, C.-C.; Klauser**,** R.; Shaporenko, A.; Grunze, M.; Zharnikov, M. *Langmuir* **2003**, *19*, 9774.

(35) Weng, C.-C.; Liao, J.-D.; Wu, Y. T.; Wang, M.-C.; Klauser**,** R.; Grunze, M.; Zharnikov, M. *Langmuir* **2004**, *20*, 10093.

(36) Pierson, J.; Czerwiec, T.; Belmonte, T.; Michel, H.; Ricard, A. *Plasma Sources Sci. Technol.* **1998**, *7*, 54.

(37) Bourg, F.; Pellerin, S.; Morvan, D.; Amouroux, J.; Chapelle, J. *J. Phys. D: Appl. Phys.* **2002**, *35*, 2281.

(38) Köhn, F. Diploma Thesis, Universität Heidelberg, Heidelberg, Germany, 1998.

(39) Heister, K.; Zharnikov, M.; Grunze, M.; Johansson, L. S. O. *J. Phys. Chem. B* **2001**, *105*, 4058.

(40) Wolf, B. H., Ed. *Handbook of Ion Sources*; CRC Press: Boca Raton, FL, 1995; Chapter 2.

(41) Grill, A. *Cold Plasma in Materials Fabrication: from fundamentals to applications*; IEEE Press: Piscataway, NJ, 1993; pp 129−137.

(42) Spanel, P. *J. Mass Spectrom. Ion Process.* **1995**, *149−150*, 299.

(43) Moulder, J. F.; Stickle, W. E.; Sobol, P. E.; Bomben, K. D. *Handbook of X-ray Photoelectron Spectroscopy*; Perkin-Elmer Corp.: Eden Prairie, MN, 1992.

(44) Lamont, C. L. A.; Wilkes, J. *Langmuir* **1999**, *15*, 2037.

(45) Heister, K.; Johansson, L. S. O.; Grunze, M.; Zharnikov, M. *Surf. Sci.* **2003**, *529*, 36.

(46) Shaporenko, A.; Ulman, A.; Terfort, A.; Zharnikov, M. *J. Phys. Chem. B* **2005**, *109*, 3898.

(47) Laibinis, P. E.; Whitesides, G. M.; Allara, D. L.; Tao, Y.-T.; Parikh, A. N.; Nuzzo, R. G. *J. Am. Chem. Soc.* **1991**, *113*, 7152.

(48) Himmelhaus, M.; Gauss, I.; Buck, M., Eisert, F.; Wöll, Ch.; Grunze, M. *J. Electron. Spectrosc. Relat. Phenom.* **1998**, *92*, 139.

(49) Ishida, T.; Hara, M.; Kojima, I.; Tsuneda, S.; Nishida, N.; Sasabe, H.; Knoll, W. *Langmuir* **1998**, *14*, 2092.

(50) Yang, Y.-W.; Fan, L.-J. *Langmuir* **2002**, *18*, 1157.

(51) Hutt, D. A.; Leggett, G. J. *J. Phys. Chem. B* **1996**, *100*, 6657.

(52) Hutt, D. A.; Cooper, E.; Leggett G. J. *J. Phys. Chem. B* **1998**, *102*, 174.

(53) Olsen, C.; Rowntree, P. A. *J. Chem. Phys.* **1998**, *108*, 3750.

(54) Huels, M. A.; Dugal, P. C.; Sanche, L. *J. Chem. Phys.* **2003**, *118*, 11168.

(55) Chenakin, S. P.; Heinz, B.; Morgner, H. *Surf. Sci.* **1998**, *397*, 84.